Relaxation dynamics in the $B(1/2)$ and $C(3/2)$ charge transfer states of XeF in solid Ar

G. J. Hoffman,[a] Dan G. Imre, R. Zadoyan, N. Schwentner,[b] and V. A. Apkarian[c]
Department of Chemistry, University of California, Irvine, California 92717

(Received 7 December 1992; accepted 1 March 1993)

Dispersed laser induced fluorescence, and time domain measurements using the optical Kerr effect are applied to study the relaxation dynamics of Xe^+F^- ($B\,^2\Sigma_{1/2}$ and $C\,^2\Pi_{3/2}$) charge transfer states in solid Ar. Very fast vibrational relaxation is observed in the C emitting site: excitation near $v=20$ leads to population of $v=0$ of the C state in 13($\pm$2) ps. In the B emitting site, the lower vibrational states relax sequentially. Relaxation times of 800($\pm$30) ps for $1\rightarrow0$ and 250($\pm$30) ps for $2\rightarrow1$, are measured directly; and 150($\pm$30) ps for $3\rightarrow2$ and <30 ps for $4\rightarrow3$ are estimated from spectral intensities. A new, much faster relaxation channel, which leads to $B(v=1$, and $v=0)$ is open to states above $v=3$ in the B emitting site. This fast channel has a relaxation time of 7($\pm$1) ps and must involve multiple internal conversions among the nested electronic states in the ionic manifold. Under intense pumping, the excited population relaxes by stimulated emission. Stimulated radiative relaxation rates larger than 1.5×10^{11} s^{-1} are observed for $B(v=0)$.

I. INTRODUCTION

As the first solid state excimer laser, XeF in solid Ar has generated interest in recent years.[1] Although previously studied,[2,3] under close scrutiny, it has become obvious that the spectroscopy of XeF in rare gas solids is not fully understood.[4] In the most recent studies it was determined that, in both Ar and Ne, XeF may occupy one of two different sites: one which emits only from the $C(^2\Pi_{3/2})$ state, and one which emits only from the $B(^2\Sigma_{1/2})$ state.[4] The XeF that emits from the C state closely resembles the gas phase molecule, though solvated by the solid medium. The excitation spectrum of the $C(^2\Pi_{3/2})\rightarrow A(^2\Pi_{3/2})$ emission shows evidence for the B state lying above the C, as is the case for XeF in the gas phase.[5] The B emitting XeF, however, appears to be highly perturbed, its ω_e increasing from the gas phase value[5] of 309 to 424 cm^{-1} in solid Ar.[4] Also, there is no obvious spectroscopic evidence for the presence of the C state in this site. Further, the vibrational bands observed in excitation while monitoring $B(^2\Sigma_{1/2})\rightarrow X(^2\Sigma_{1/2})$ emission show a strong, specific coupling to both bulk and local phonon modes. Based on the absence of emission from the C state, it is inferred that C lies above the bottom of the B in this case, in contrast with the gas phase ordering of states. This unusual site dependence of energetics has been difficult to explain. The possibilities that the B emitting site is perturbed by an additional F atom (FXeF), or by an additional Xe (linear XeXeF), or by a nearby XeF (XeF dimer) have been considered without reaching a firm conclusion.[4] Thus the exact nature of the solid state XeF($B\rightarrow X$) laser remains the subject of research. In the present paper, we will treat the B emitter as a strongly perturbed diatomic XeF.

XeF in the ground state is the most deeply bound of rare gas halides. As such, it can be effectively thought as an isolated diatomic in lighter rare gas solid hosts. The stability of XeF(X) is ascribed to the partial charge transfer character borrowed mainly from the excited ionic $B(^2\Sigma_{1/2})$ state. Due to the ionic admixture from excited charge transfer states, the ground state acquires a dipole of 1.2 D.[6] In contrast, the excited ionic states are the result of a full charge transfer from Xe to F, and accordingly are characterized by giant dipoles of $\sim$12 D.[6] This consideration makes the studies of relaxation dynamics in this system rather fascinating. We expect the charge transfer states to be strongly coupled to the lattice, and the spectroscopy of the system makes this amply clear.[4] As mentioned above, to rationalize the spectroscopic details, it has been necessary to consider site perturbations explicitly. The time domain measurements reinforce these considerations. Combining the spectroscopic information with direct time domain measurements, in an effort to provide a detailed description of charge transfer relaxation dynamics in this model system, is the motivation of the present work.

Numerous studies on excited state relaxation dynamics of diatomic molecules trapped in rare gas solids can be found in the literature. Examples range from early laser induced fluorescence experiments on NH and ND,[7] OH [8,9] and OD,[8] C_2 [10] and C_2^-,[11] and CN,[12,13] to more recent studies using synchrotron radiation on CO [14] and NO.[15,16] A rather complete review of vibrational relaxation dynamics in these systems was presented by Dubost, and remains a valid picture of the existing understanding.[17] In the case of isolated vibrational levels, which is a situation more commonly encountered in the electronic ground state of molecules, the required multiphonon relaxation in these systems is inherently an inefficient process. The fastest reported lifetimes are in the range of $10^{-9}\sim10^{-8}$ s.[17] The situation is quite different in the case of relaxation in nested electronic potentials, classic examples of which are C_2, C_2^-, CN, and CO. In these systems vibrational energy flows via distinct pathways involving internal conversions

[a]Present address: Department of Chemistry, Willamette University, 900 State St., Salem, OR 97301.
[b]Permanent address: Institut für Atom und Festkörperphysik, Freie Universität Berlin, 1000 Berlin 33, Germany.
[c]Alfred P. Sloan fellow; to whom correspondence should be addressed.

 0021-9606/93/129233-08$06.00

and intersystem crisscrossings. Although the resulting relaxation pathways can be very complicated, they can be predicted following the laws of minimum energy gap, maximum Frank–Condon overlap, and favorable electronic coupling elements.[14] Lattice phonons mediate the relaxation, and provide the energy conservation conditions.[11,14] The Rydberg $A(^2\Sigma^+)$ (Ref. 15) and $C(^2\Pi)$ (Ref. 16) states of NO is a typical example that parallels the presently studied system. There, it has been clearly shown that the rare gas matrix environment influences the relaxation cascade in these states by coupling them to nearby valence states. Lifetimes of individual vibrational levels are found to be of order 10^{-9} s or shorter. However, in selected molecule-matrix combinations the cascade usually passes through bottlenecks—isolated vibrational levels with lifetimes of 10 ns to 10 ms—which slow the process down, and strongly extend overall vibrational relaxation times.

The B and C states of XeF are nested in a fashion similar to the excited states of some of the molecules discussed above. Moreover, due to the change in dipole of order 10 D between excited and ground states, strong coupling of the excited states to acoustic modes of the lattice may be expected. Incipient bonding to Ar atoms in the excited state, and therefore the creation of strongly coupled local phonon modes is also possible. The mixed triatomic exciplexes $(RgRg')^+X^-$ are well known in the gas phase, and it has been recognized that a delicate balance in energetics of the diatomic and mixed triatomic configurations exist in the condensed phases.[18] In the case of XeF doped solid Ar, the diatomic configuration is the lowest energy charge transfer state. This is explained by the fact that the binding energy of $(XeAr)^+$ of 0.176 eV (Ref. 19) is comparable to the cohesive energy of the host lattice. Nevertheless, vibrationally excited states of the diatomic can in principle couple to the lattice through the metastable triatomic coordinate. In short, one might expect to see very fast vibrational relaxation in these charge transfer states due to effective coupling to both lattice and local phonon modes, and due to the fact that vibrational frequencies in XeF correspond to $\sim$5 matrix phonons. Subnanosecond relaxation by direct coupling into the phonon bath or by crisscrossing between potential surfaces is predictable. This is, in fact, what we observe for the C emitting species, which relaxes very quickly (13 ps). The B emitting site shows more complex relaxation dynamics. Depending on the originally excited vibrational level, the molecule may relax very quickly (7 ps) or relatively slowly ($\sim$1 ns).

II. EXPERIMENT

All of the studies to be reported here were conducted in free-standing crystals prepared from 1:1:3000 gaseous mixtures of Xe and F_2 in Ar. The method of preparing such crystals has been outlined in detail previously.[20] XeF emission is observed after irradiating the sample with either 308 nm light (from a XeCl excimer laser) or 355 nm light (from a Nd:YAG laser) while keeping the crystal at a temperature of 25 K. The ultraviolet light efficiently dissociates the F_2. The resulting F atoms at the elevated temperature can thermally diffuse through the solid Ar (Ref. 21) until finding a Xe, thus producing XeF. After a sufficient amount of XeF emission is observed (typically after 30 to 45 min of irradiation), the temperature of the crystal is lowered to the bottom temperature of the cryostat (15 K).

For the spectroscopic measurements, the light source is an excimer pumped nanosecond dye laser (Lambda Physik EMG 101 MSC/FL2002). The sample fluorescence is dispersed through a 0.75 m monochromator (Spex 1702), detected by a photomultiplier, and recorded by a computer controlled digital oscilloscope (Tektronix 2430 or 2440) operating as a boxcar.

The time domain measurements are obtained using the optical Kerr effect in a cell of CS_2 to monitor the luminescence produced by the sample as a function of delay after excitation.[22] In these studies, the light source is a cw mode-locked Nd:YAG laser (Coherent Antares 76 YAG, 1064 nm, 76 MHz, 70 ps, 30 W) frequency doubled (532 nm, 60 ps, 2 W) to synchronously pump an ultrafast dye laser operating at $\sim$640 nm (Coherent Satori, using Kiton Red as the gain medium and malachite green as the saturable absorber). The dye laser pulses typically have autocorrelations of 120–150 fs and energies of a few nJ. A small amount of the fundamental from the mode-locked YAG is picked off and set to a regenerative amplifier (Continuum RGA60) operating at 30 Hz. When doubling only, the 532 nm pulse energy is typically 30 mJ; when simultaneously doubling and tripling, 532 nm pulses have an energy of 20 mJ, while the 355 nm pulses have an energy of 5 mJ. The doubled pulses are used to pump a pulsed dye amplifier that amplifies the femtosecond 640 nm pulses. While preserving the autocorrelation length of the input pulses, the output pulses have energies as high as 1 mJ. These pulses can be doubled through a 1 mm long BBO crystal to produce short pulses at $\sim$320 nm with energies of 10 μJ and approximately 200–250 fs duration.

The experimental setup for the Kerr effect measurements is shown in Fig. 1. Depending on the experiment, pulses of either 320 or 355 nm excite the sample while delayed 640 nm pulses are used to switch on the CS_2 shutter. The signal is collected colinearly with excitation and sent to the Kerr cell, which is a 2 cm cell filled with CS_2 between two crossed Glan–Thompson polarizers. The delay of the 640 nm pulses is varied using a 1 m long delay stage with a time resolution of 0.66 ps (Klinger), and its polarization is optimized for detection of the Kerr signal by a $\lambda/2$ retarder. The time resolution of the experiment itself is 2 ps, due to the relaxation time of the CS_2.[22] The light transmitted through the crossed polarizers is filtered through a notch filter (either 410 or 520 nm depending on whether $B \rightarrow X$ or $C \rightarrow A$ is being detected), dispersed by a $\frac{1}{4}$ m monochromator (McPherson), detected by a photomultiplier (Hamamatsu R943-02), and recorded and averaged by a computer reading the signal through a boxcar integrator (SRS).

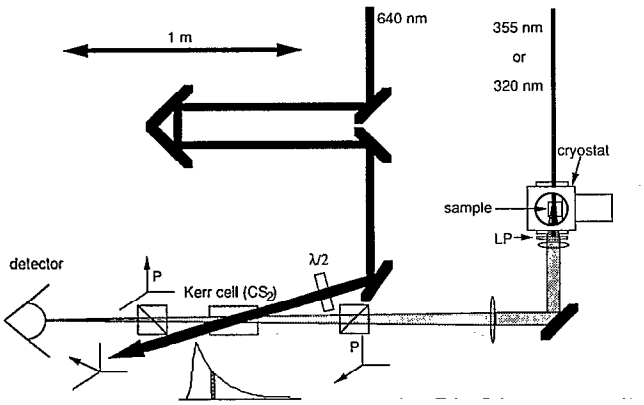

FIG. 1. Experimental setup for optical Kerr effect measurements. Emission is collected colinearly with excitation; after passing through the sample, the residual pump laser light is blocked by a 385 nm long-pass filter (LP). Sample fluorescence is collimated and sent through a 2 cm long cell of CS_2 placed between two crossed polarizers. The 100 fs 640 nm pulses are sent through a variable delay line and a half-wave plate before overlapping the sample fluorescence in the CS_2 cell. Using the half-wave plate, the polarization of these pulses is adjusted to 45° from the orientation of the polarizers, which maximizes the Kerr effect signal. The Kerr shutter provides that only fluorescence from a ~2 ps gate has its polarization rotated enough to pass through the second polarizer; this is represented in the sketch below the CS_2 cell.

III. RESULTS AND DISCUSSION

A. Spectroscopic data

Both emission and excitation spectra of the $B \rightarrow X$ transition of XeF in solid Ar have been reported elsewhere.[4] The maximum of the emission spectrum has been assigned to the $v'=0$ to $v''=1$ transition. In addition, emission from vibrationally excited states has been clearly identified, specifically, from $v'=1$, 2, and 3. The contribution from these bands to the overall emission spectrum is seen to increase when successively higher v' states are accessed, the implication being that each vibrational level relaxes to the one lying below it within the B manifold. However, the emission spectrum obtained by exciting to $v'=4$, when normalized to the maximum of the spectrum obtained by exciting to $v'=3$, shows a dramatic decrease in emission from these vibrationally excited states (see Fig. 2). Emission from $v'=1$ is reduced by approximately 50%; that from $v'=2$ and 3 decreases by 80%. A new, apparently fast channel opens at $v'=4$ whereby the molecules can relax back to $v'=0$, and to a lesser extent to $v'=1$, without passing through $v'=2$ or 3.

Figure 3 compares excitation spectra obtained by monitoring emission from $v'=0$, 1, and 2. The figure clearly shows the drop in intensity of emission from $v'=1$ and 2, when states at $v'=4$ and above are excited. The vibrational energy flow in the B manifold can be extracted from such a series of spectra. Defining $I_n(v')$ as the emission intensity from state n, when state v' is initially excited; we recognize that the ratio

$$F_n(v') = \frac{I_n(v')/I_n(3)}{I_0(v')/I_0(3)} \qquad (1)$$

gives the fraction of molecules relaxing through vibrational level n when initially excited to vibrational level v'. In Eq. (1), the assumption that the vibrational population will accumulate in $n=0$ is made, and vibrational level 3 is chosen to normalize the relative intensities because it is the last and most intense band in the excitation spectrum before the new channel opens. Figure 4 plots $F_1(v')$ and $F_2(v')$. Because both $n=2$ and $n=3$ emissions decrease by the same amount on going from $v'=3$ to $v'=4$ (Fig. 2), it is apparent for both excitations that the molecules in the $n=2$ state got there from $n=3$. Thus $F_2(v')$ represents the

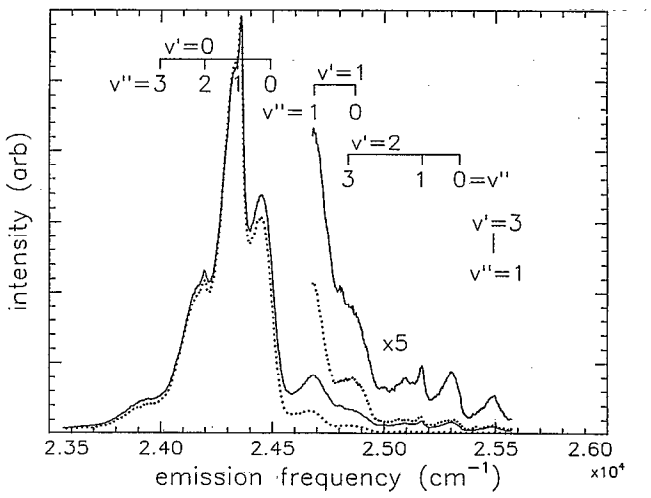

FIG. 2. Assigned $B \rightarrow X$ emission spectra for XeF excited to $B(v'=3)$ (solid line), and $B(v'=4)$ (dotted line) scaled to the maxima. Note the decrease in emission from excited vibrational states on going from $v'=3$ to $v'=4$.

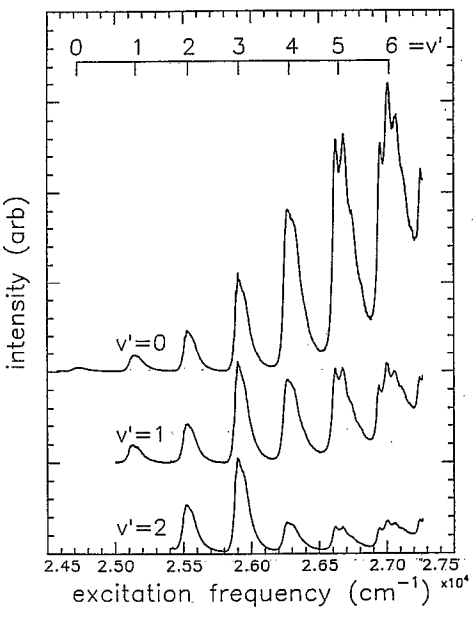

FIG. 3. Assigned $B \rightarrow X$ excitation spectra for emission from $v'=0$ (top, $\lambda_{obs}=410.6$ nm [24 355 cm^{-1}]), $v'=1$ (middle, $\lambda_{obs}=405.0$ nm [24 691 cm^{-1}]), and $v'=2$ (bottom, $\lambda_{obs}=397.5$ nm [25 157 cm^{-1}]). At $\lambda=405.0$ nm, there is substantial overlap between the $v'=1$ and $v'=2$ emissions, necessitating subtraction of a component of the $v'=2$ excitation spectrum from that observed at $\lambda=405.0$ nm.

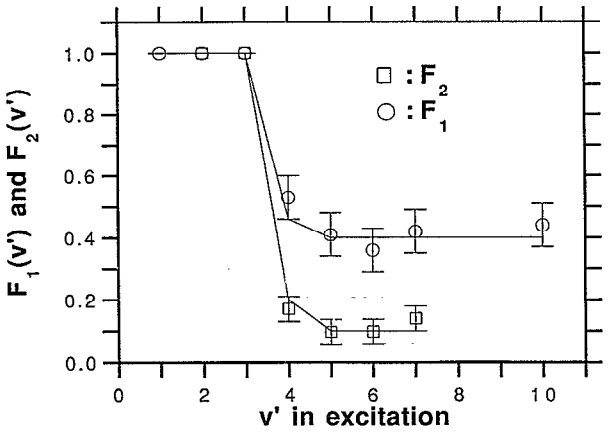

FIG. 4. Fraction of molecules relaxing through $n=1$ and $n=2$ as a function of v' in excitation. There is a large drop for both at $v'=4$, and a second, smaller drop at $v'=5$. For $v'>5$, the fraction stays constant. The lines show what behavior would be expected from the model presented in Sec. III B 1.

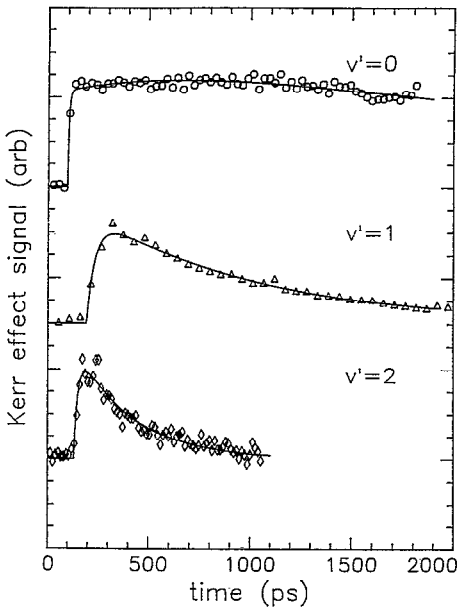

FIG. 5. Time dependence of the emission from $v'=0$ (top, 320 nm excitation), $v'=1$ (middle, 355 nm excitation), and $v'=2$ (bottom, 355 nm excitation) as measured using the Kerr shutter. The $v'=0$ emission is fit to two exponential rises, one with $\tau_r=7$ ps, and one with $\tau_r=800$ ps, and a fall time of 2.9 ns; the only variable parameter, the fraction for the rise with $\tau_r=800$ ps, was returned by the fit as 0.46, consistent with the results from the excitation spectra to within experimental error. The fall time of the $v'=1$ emission is 800 ps; the fall time of the $v'=2$ emission is 250 ps.

fraction of molecules that relax within the B manifold. At $v'=4$, this is approximately 20% of what would be expected if all the molecules relaxed through $n=2$ [i.e., $F_2(4)\approx 0.2$], implying that 80% bypass the B vibrational ladder. If the only source of $n=1$ population was relaxation from $n=2$, the $n=1$ emission ought to be reduced by 80% also. Instead, it is reduced by just 50% [$F_1(4)\approx 0.5$]; i.e., half of the molecules excited to $v'=4$ pass through $n=1$. Since 20% will pass through $n=1$ anyway, relaxing from $n=2$, this implies that 30% come back to $v'=1$ from the relaxation channel outside the B manifold. Clearly, the remaining 50% of the molecules in this channel relax directly to $n=0$. Thus, of the molecules that relax by bypassing the B manifold, according to the $v'=4$ excitation data, 40% return to the B manifold in $n=1$, and 60% return to $n=0$. For excitation to $v'\geqslant 5$, $n=1$ emission is reduced to approximately 40% of what would be expected if all molecules passed through $n=1$ [$F_1(v'\geqslant 5)\approx 0.4$], and $n=2$ emission is similarly reduced to about 10% [$F_2(v'\geqslant 5)\approx 0.1$]. This implies that the $v'=5$ state splits in relaxation by about 50% between $n=4$ of the B manifold and the fast channel. (Knowing that 20% of the molecules that make it to $n=4$ of the B state continue to relax within the B manifold, and seeing 10% pass through $n=2$, leads to the conclusion that only 50% of the molecules excited to $v'=5$ relax to $n=4$.) In any case, for $v'=5$ and above, relaxation within the B manifold appears to be just as fast as the fast channel outside the B manifold. Also, for $v'\geqslant 5$, the ratio of return via the fast channel to $n=1$ vs $n=0$ is about 30% to 70%. The return ratio from $v'=10$, shown in Fig. 4, is obtained by stimulated gain measurements in which 355 nm is used as pump while the amplification of white light is monitored by the OMA. Stimulated emission from both $v'=1$ and $v'=0$ can be seen, and using the known relaxation rates of these states (see next section) their relative populations could be directly extracted. Within experimental error, reasonable agreement to the data is achieved for *all* peaks above $v'=3$ if one assumes a return ratio of 1:2 for $n=1$ to $n=0$ by the fast channel.

The drop in emission from vibrationally excited states is not the only change that occurs in the excitation spectrum at $v'=4$. As has been noted,[4] for $v'=1$, 2, and 3, there is a 15 cm^{-1} phonon progression present on the excitation peaks; at $v'=4$, this progression disappears and is replaced by a 55 cm^{-1} progression. The frequency in the higher energy progression corresponds closely to the Debye limit in Ar (65 cm^{-1}).[23] Apparently, there is a significant change in the dynamics of the B state at $v'=4$. The ability of the molecule to couple efficiently with high frequency phonon modes of the solid above $v'=4$ may in part explain the different relaxation rates above and below $v'=4$.

While the C emitting XeF site in both Ar and Ne show evidence for the B state lying above the C, the B emitting site shows no obvious spectroscopic clues for the location of the C state.[4] Nonetheless, if we restrict ourselves to the diatomic exciplex model, the C state must be nearby. The opening of a new relaxation channel at $v'=4$, suggests that the C state crosses the B state near $v'=4$ or 5. The return of this population to $v'=0$ of B, suggests that the bottom of the C state lies just slightly above $v'=0$ of the B state. This would provide a mechanism for the fast relaxation outside the B manifold and an avenue for return. This point will be further developed in light of the time-dependent data below.

B. Time-resolved data

1. Relaxation within the B manifold

Figure 5 shows the time dependence of fluorescence from $v'=0$ (410.6 nm, 24 355 cm^{-1}), $v'=1$ (402.0 nm,

24 876 cm^{-1}), and $v'=2$ (397.5 nm, 25 157 cm^{-1}), as measured by the Kerr effect signal, as a function of time. The $v'=0$ measurement was done using 320 nm excitation; the $v'=1$ and 2 measurements used 355 nm excitation as the 320 nm pump was not intense enough to allow observation of $v'=1$ and 2 emissions. The last two profiles show fits to the functional form:

$$I(t)=\begin{cases}\dfrac{\tau_r\tau_f}{\tau_r-\tau_f}\left[\exp\left(-\dfrac{(t-t_0)}{\tau_r}\right)-\exp\left(-\dfrac{(t-t_0)}{\tau_f}\right)\right], & t\geqslant t_0\\ 0, & t<t_0\end{cases}, \tag{2}$$

where τ_r and τ_f are the rise and fall times of the emission. Equation (2) should be recognized as the response function of the intermediate state in a two step sequential kinetic scheme. The fit for $v'=1$ gives $\tau_f=800\pm30$ ps, and for $v'=2$, $\tau_f=250\pm30$ ps. In the 2 ns period shown here, the $v'=0$ emission appears not to be changing at all. In fact, beside the very fast rise from the fast channel, there is a slow rise due to relaxation from $v'=1$ on top of the radiative exponential fall. The radiative lifetime of the B state was measured using a photodiode with a 350 ps fall time (Electro-Optics Technology ET 2000) and a transient digitizer (Tektronix DSA 602 with 1 GHz bandwidth) to be 2.9 ± 0.5 ns. To describe the time evolution of the $v'=0$ level, the fact that two independent sources feed into it need be taken into account. Accordingly, the $v'=0$ emission profile is fit to the function:

$$I(t)=\begin{cases}(1-\alpha)\exp\left(-\dfrac{(t-t_0)}{\tau_{r1}}\right)+\alpha\exp\left(-\dfrac{(t-t_0)}{\tau_{r2}}\right)-\exp\left(-\dfrac{(t-t_0)}{\tau_f}\right), & t\geqslant 0\\ 0, & t<t_0\end{cases}, \tag{3}$$

where α is the fraction that relaxes to $v'=0$ from $v'=1$. Setting $\tau_f=2.9$ ns, $\tau_{r1}=7$ ps (see below), and $\tau_{r2}=800$ ps gives the fit shown, with a value for $a=0.46$, which matches the expected F_1 from the model presented in the previous section to within experimental error.

In principle, the rise of both the $v'=1$ and the $v'=2$ emissions ought to contain the lifetimes of the $v'=2$ and $v'=3$ emissions, respectively. However, in the case of the $v'=1$ rise, there is a great deal of overlap between the $v'=1$ and 2 emissions, making such an interpretation of the rise impossible. Moreover, when excited at 355 nm, the contribution to population from the fast channel is expected to mask the sequential kinetics. In both cases, the rise time is on the order of the laser pulse width ($\sim$50 ps). The decays are single exponential, and as such appear to purely correspond to $v'=1$ and $v'=2$.

The time dependence of fluorescence from $v'=3$ was not directly measured, but from comparison of the intensities of $v'=3$ emission to the $v'=2$ emission, the lifetime of $v'=3$ is estimated to be 100–200 ps.

2. Relaxation via the fast channel

Figure 6 shows examples of rises for both the $B(v'=0)\rightarrow X$ and $C\rightarrow A$ emissions using 320 nm excitation from Kerr effect measurements. The risetime for the $B\rightarrow X$ is 7 ± 1 ps; that for the $C\rightarrow A$ is 13 ± 2 ps. In the case of the $B\rightarrow X$ emission, the molecule must lose more than 6600 cm^{-1} in energy to reach $v'=0$ of the B, yet this occurs in only 7 ps. Likewise, the C emitting site is excited to 5600 cm^{-1} above $v'=0$ of the C state and gives up that energy to its surroundings in just 13 ps. This implies that the C state couples very efficiently to phonons, and it supports the notion that the fast relaxation channel for the B emitting site is mediated by the C state.

An overall scheme summarizing the relaxation routes of the B emitting XeF in Ar is presented in Fig. 7. When the molecule is excited above $v'=4$, it relaxes very quickly either by efficient vibrational relaxation within the B manifold, or by cascading between the B manifold and the fast

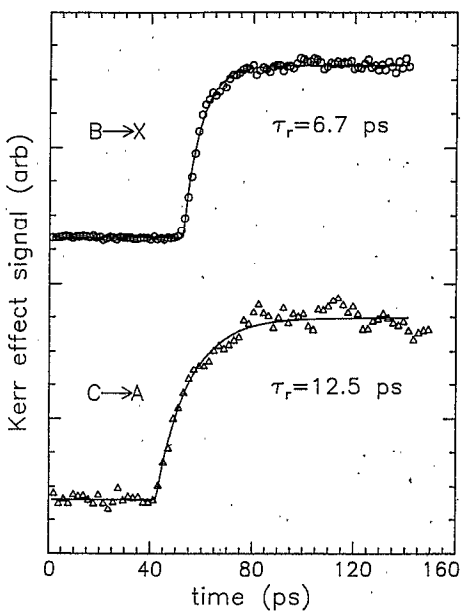

FIG. 6. Examples of time profiles of the $B\rightarrow X$ (top) and $C\rightarrow A$ (bottom) emissions using 320 nm excitation measured using the Kerr shutter. The $B\rightarrow X$ gives an average rise time of 7 ps; the $C\rightarrow A$ gives an average risetime of 13 ps.

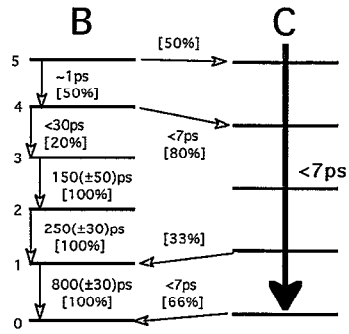

FIG. 7. Diagram showing the possible modes of relaxation for the B emitting XeF. The fast channel opened at $v'=4$ and 5 in the B manifold may be caused by a resonance of the B potential with the C potential at that energy.

channel (presumably the C manifold) though it should be emphasized that all relaxation is fast at these energies. By the time the molecule has relaxed to the energy of $v'=4$ in the B, approximately half of the molecules are in the B manifold (i.e., $v'=4$) and half are in the fast channel. The lifetime of the $v'=4$ state is constrained by the lifetime of the overall relaxation process to be <7 ps. Given that the branching ratio for going to the fast channel (τ_{4-c}) vs $v'=3$ (τ_{4-3}) is 4 to 1, one can put upper limits on the relaxation times for each of these pathways. Using the relations

$$\frac{1}{\tau_{4-c}}+\frac{1}{\tau_{4-3}}>\frac{1}{7\ \text{ps}} \tag{4}$$

and

$$\frac{1/\tau_{4-3}}{1/\tau_{4-c}+1/\tau_{4-3}}=0.2 \tag{5}$$

one obtains the limits $t_{4-c}<9$ ps, and $t_{4-3}<36$ ps. The molecules in the fast channel relax in 7 ps to $v'=1$ and $v'=0$ with a ratio of approximately 1 to 2, while the 10% in $v'=3$ slowly climb down the B vibrational ladder.

The observed energy flow pathways are collected in the map given in Fig. 7. The vibrational spacing in the B manifold is well characterized spectroscopically. Near the bottom of the potential they are well fit by a harmonic frequency of $\omega_e=424\ \text{cm}^{-1}$, and anharmonicity of $\omega_e x_e=7.5\ \text{cm}^{-1}$.[4] However, as discussed in the introduction, there are no spectroscopic observations relating the C state in the B emitting site. The C state vibrational levels shown in Fig. 7, a harmonic ladder of $\omega_e=450\ \text{cm}^{-1}$, represents a guess based on the observed relaxation kinetics, and with minimal assumptions. The basis is as follows. Since only B emits here, the C state must be above B. Since population returns to $B(v=0)$ on a time scale of 7 ps, the $C(v=0)$ must lie within one phonon. We therefore place the $C(v=0)$ state 50 cm^{-1} above B. The gas phase vibrational frequency of the C state exceeds that of the B by $\sim 10\%$. Assuming that this ratio is maintained in the matrix as well, a vibrational frequency of $\sim 450\ \text{cm}^{-1}$ can be justified in the B emitting site. This would also provide a two-phonon return channel from $C(v=1)$ to $B(v=1)$, consistent with the observation that a significant fraction of the population in the fast channel returns to $B(v=1)$. The scheme also produces the requisite isolation of $v=2$ and $v=3$ in B from nearby states (by three or more phonons). Finally, $B(v=4)$ approaches $C(v=3)$ and $B(v=5)$ becomes nearly resonant with $C(v=4)$, providing entrances into the fast channel. Based on energy gaps alone, this minimal model provides paths for fast exit from B near $v=4$, and a fast channel for return near $v=0$. Furthermore, the observed decay rates, for $v=4$ through $v=1$ of B, show an exponential energy gap law if we were to assume that the decay from each state proceeds via the nearest exoergic vibrational channel of either electronic surface. In the absence of electronic mixing coefficients, or direct spectroscopic information about the C state, a more quantitative analysis of the observed decay rates would be superfluous.

For the above model to hold, vibrational relaxation in the C state has to be much faster than in the B state. Fast vibrational relaxation, 13 ps, in the C emitting site was already noted. The disparity in relaxation times of ~ 2 orders of magnitude between the C state vibrational levels and the lowest states in the B manifold is remarkable. This difference in behavior may originate from the difference in symmetries of the two electronic states: Π for C and Σ for B. Significantly stronger coupling of molecular Π states (or atomic P states) to the surrounding lattice has been documented in prior studies of impurities, CO (Ref. 24) and He (Ref. 25) are examples. This difference has been attributed to the stronger anisotropy of guest–host interactions. The experimental observation that in excitation spectra the phonon contour lines in the C state are broadened and structureless, while in the B state they are well resolved, is consistent with the above picture. We take a more specific view of coupling to local phonons, by considering the mixed triatomic exciplex coordinate, namely the local minimum that can be ascribed to $(\text{ArXe})^+\text{F}^-$. There is a significant distinction between the $B(\Sigma)$ and $C(\Pi)$ states with this respect: The Π state correlates with the lowest triatomic ionic state.[6] It may therefore be possible to imagine that while the C state is always coupled to the lattice through the XeAr^+ coordinate, that the B state may actually become pure diatomic only near the bottom of its potential. While this picture is somewhat appealing, it does not explain why there should be a switch in the ordering of B and C states in different sites.

3. Measurement of the $B\rightarrow X$ (410.6 nm) laser

Under high intensity pumping by 355 nm ($\sim 10^9$ W cm^{-2} and greater), lasing of the $B\rightarrow X$ transition was apparent. Observing the time dependence of the laser using the CS_2 Kerr cell revealed that the radiative lifetimes of the B state are controlled by stimulated emission rates. Figure 8 shows time profiles of the $B\rightarrow X$ laser for 355 pump power increasing from top to bottom. To determine the fall time for the shortest pulses, it was necessary to fit to a convolution of the 52 ps 355 nm pulse (assumed to be Gaussian) with the functional form of Eq. (2) using the

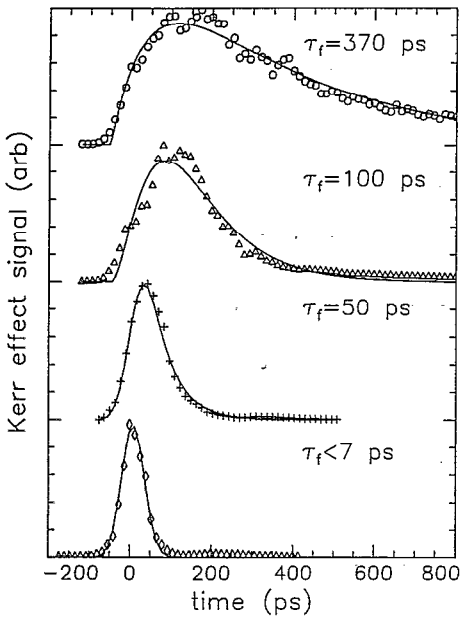

FIG. 8. Time dependence of $B \rightarrow X$ emission for increasing pump power at 355 nm. The decreasing falltime indicates the onset of lasing. The two shortest pulses require convolutions with the pump pulse profile to extract a fall time; the shortest pulse has a falltime shorter than the 7 ps rise.

known rise time of 7 ps and a variable fall time. For the shortest of the pulses, the fall time returned by the fit was 2 ps, i.e., shorter than the rise time; in such a case, the rise time and the fall time temporally appear to trade places [see Eq. (2)]. This determination cannot be regarded as reliable, as attempting to extract a fall time more than one order of magnitude smaller than the pulse from which it is being deconvoluted ought not give a true value. It is, however, clear that under these conditions, the stimulated radiation rate of the B state is limited by the pump pulse width. It was however surprising that the 800 ps feed rate from $v=1$ was not apparent. The two slower time profiles of Fig. 8 were fit to Eq. (2) without convolution to the laser pulse. Both show the rise time for the emission to be slowing. At least a portion of the rise is significantly slower than the 50 ps pump pulse width, but not as slow as the 800 ps $v'=1$ relaxation time. One plausible explanation for these observations is the shortening of the $v'=1$ relaxation time due to its lasing. A small but significant portion of the $v'=1$ emission overlaps with the lasing transition of the $v'=0$, and thus can have its emission to the ground state stimulated as well. However, this is only speculation. Degradation of the sample under intense pumping conditions makes quantitative studies of lasing on picosecond time scales of this system difficult. We note that the prior studies of the solid state XeF laser have utilized ns pulses, and therefore must have involved significant population cycling. This situation is similar to the case of C–A lasing in a cavity, which has recently been treated in a report.[26] The present estimates of gain cross sections, and conversion efficiency remain in good agreement with the prior determinations based on spectral narrowing measurements.[1]

IV. CONCLUSIONS

Results of experiments revealing the vibrational relaxation dynamics of the B and C charge transfer states of XeF in solid Ar have been presented. For the C emitting species, the rise time for relaxed emission is 13 ps, which implies very fast vibrational relaxation. The B emitting species, on the other hand, shows evidence of more complex dynamics. Relaxation near the bottom of the B manifold is found to be relatively slow. The $1 \rightarrow 0$ lifetime of 800 ps, is quite comparable to other systems of similar energy gap: $CuO(B\,^2S)$ shows a relaxation time ~ 1 ns for an energy gap of 624 cm^{-1}, and $S_2(B\,^3S_u^-)$ relaxes on ~ 10 ns, for a vibrational gap of 454 cm^{-1}.[17] Thus, the giant dipole of the Xe^+F^- does not seem to have led to a much stronger coupling to phonons. We observe the $2 \rightarrow 1$ relaxation rate to be 250 ps, and we estimate $3 \rightarrow 2$ to have a lifetime of approximately 100–200 ps. The strong dependence of these relaxation rates on vibrational quantum numbers can be attributed to anharmonicities, and to the generally expected linear scaling of rate constants with vibrational quantum numbers.[27,28] Above $v'=4$, a fast channel for relaxation opens up, and $v'=1$ and 0 are populated with a rise time of 7 ps and with a ratio of approximately 1:2; however, there is still significant branching (10%) into the slower relaxation mode, down the vibrational ladder of the B manifold. The fast channel may be ascribed to a crossing from the B to the C manifold, which can then return the population back to the B manifold once it has reached the bottom of the C. This aspect is rationalized by a qualitative energy level scheme that was presented.

The short emission rise time in the C emitting state and the fast channel of the B emitting site requires very strong coupling to phonons. Such a coupling is clearly apparent in the $B \rightarrow X$ excitation spectrum for $v' > 4$, where a progression with a frequency of 55 cm^{-1} begins, and in the $C \rightarrow A$ excitation spectrum,[4] where the vibrational levels of the C state are broadened almost to the point of coalescence, and no vibrational structure can be discerned after the onset of the B state. These observations lead to the conclusion that the C state, which has predominantly Π symmetry, is more strongly coupled to the lattice than the B state, which is predominantly Σ. The trend is justifiable based on a general consideration of the anisotropy of guest–lattice potentials. More specifically, the Π state is expected to be more strongly coupled to the lattice in the present case via the triatomic charge transfer configuration $(ArXe)^+F^-$ since it correlates directly with the lowest lying $4^2\Gamma$ configuration.[6]

ACKNOWLEDGMENTS

This research was supported by the US Air Force Phillips Laboratory under Contract No. S04611-90-K-0035; by a grant from the National Science Foundation, ECS-8914321; and by the University of California, Irvine through an allocation of computer resources.

[1] N. Schwentner and V. A. Apkarian, Chem. Phys. Lett. **154**, 413 (1989).
[2] J. Goodman and L. E. Brus, J. Chem. Phys. **65**, 3808 (1976).

[3] B. S. Ault and L. Andrews, J. Chem. Phys. **65**, 4192 (1976).
[4] G. Zerza, G. Sliwinski, N. Schwentner, G. Hoffman, D. Imre, and V. A. Apkarian (unpublished).
[5] H. Helm, D. L. Huestis, M. J. Dyer, and D. C. Lorents, J. Chem. Phys. **79**, 3220 (1983).
[6] P. J. Hay and T. H. Dunning, J. Chem. Phys. **69**, 2209 (1978).
[7] V. E. Bondybey and L. E. Brus, J. Chem. Phys. **63**, 794 (1975); J. Goodman and L. E. Brus, *ibid.* **65**, 3146 (1976).
[8] L. E. Brus and V. E. Bondybey, J. Chem. Phys. **63**, 786 (1975).
[9] J. Goodman and L. E. Brus, J. Chem. Phys. **67**, 4858 (1977).
[10] V. E. Bondybey, J. Chem. Phys. **65**, 2296 (1976).
[11] V. E. Bondybey and L. E. Brus, J. Chem. Phys. **63**, 2223 (1975).
[12] V. E. Bondybey, J. Chem. Phys. **66**, 995 (1977).
[13] V. E. Bondybey and A. Nitzan, Phys. Rev. Lett. **38**, 889 (1977).
[14] J. Bahrdt and N. Schwentner, J. Chem. Phys. **88**, 2869 (1988).
[15] M. Chergui, R. Schriever, and N. Schwentner, J. Chem. Phys. **89**, 7083 (1988); M. Chergui and N. Schwentner, *ibid.* **91**, 5993 (1989).
[16] M. Chergui, N. Schwentner, and V. Chandrasekharan, Phys. Rev. Lett. **66**, 2499 (1991); J. Chem. Phys. **97**, 2881 (1992).
[17] H. Dubost, in *Inert Gases*, Springer Series in Chemical Physics, edited by M. L. Klein (Springer-Verlag, New York, 1984).
[18] H. Kunttu, E. Sekreta, and V. A. Apkarian, J. Chem. Phys. **94**, 7819 (1991).
[19] Y. C. Yu and D. W. Setser, J. Phys. Chem. **94**, 2934 (1990).
[20] W. G. Lawrence and V. A. Apkarian, J. Chem. Phys. **97**, 2224 (1992).
[21] J. Feld, H. Kunttu, and V. A. Apkarian, J. Chem. Phys. **93**, 1009 (1990).
[22] M. A. Duguay and J. W. Hansen, Appl. Phys. Lett. **15**, 192 (1969); M. A. Duguay and J. W. Hansen, Opt. Commun. **1**, 254 (1969).
[23] B. M. Powell and G. Dolling, in *Rare Gas Solids*, edited by M. L. Klein and J. A. Venables (Academic, London, 1977), Vol. II.
[24] J. Bahrdt, P. Gurtler, and N. Schwentner, J. Chem. Phys. **86**, 6108 (1987).
[25] For a review see, N. Schwentner, E. E. Koch, and J. Jortner, in *Electronic Excitations in Rare Gas Solids* (Springer, Heidelberg, 1985).
[26] G. Zerza, G. Sliwinski, and N. Schwentner, Appl. Phys. B **55**, 331 (1992).
[27] A. Nitzan, S. Mukamel, and J. Jortner, J. Chem. Phys. **63**, 200 (1975).
[28] D. Diestler, J. Chem. Phys. **60**, 2692 (1974).